From Cu(I) and Cu(I)-Cu(II) mixed-valence clusters to 2D Cu(II) and Cu(I) coordination polymers supported by a flexible bis-tetrazole organosulfur ligand.

Olaya Gómez-Paz[a,b], Rosa Carballo[a,b*], Ana B. Lago[c*], Inmaculada Prieto[b,d], Ezequiel M. Vázquez-López[a,b].

a Universidade de Vigo, Departamento de Química Inorgánica, Facultade de Química, 36310 Vigo, Spain

b Metallosupramolecular Chemistry Group, Galicia Sur Health Research Institute (IIS Galicia Sur). SERGAS-UVIGO, Galicia, Spain

c Departamento de Química, Facultad de Ciencias, Sección Química Inorgánica, Universidad de la Laguna, 38206 La Laguna, Spain

d Universidade de Vigo, Departamento de Química Física, Facultade de Química, 36310 Vigo, Spain

***Correspondence e-mail: alagobla@ull.edu.es**

Supplementary material

Contents: **Page**

1. Characterization

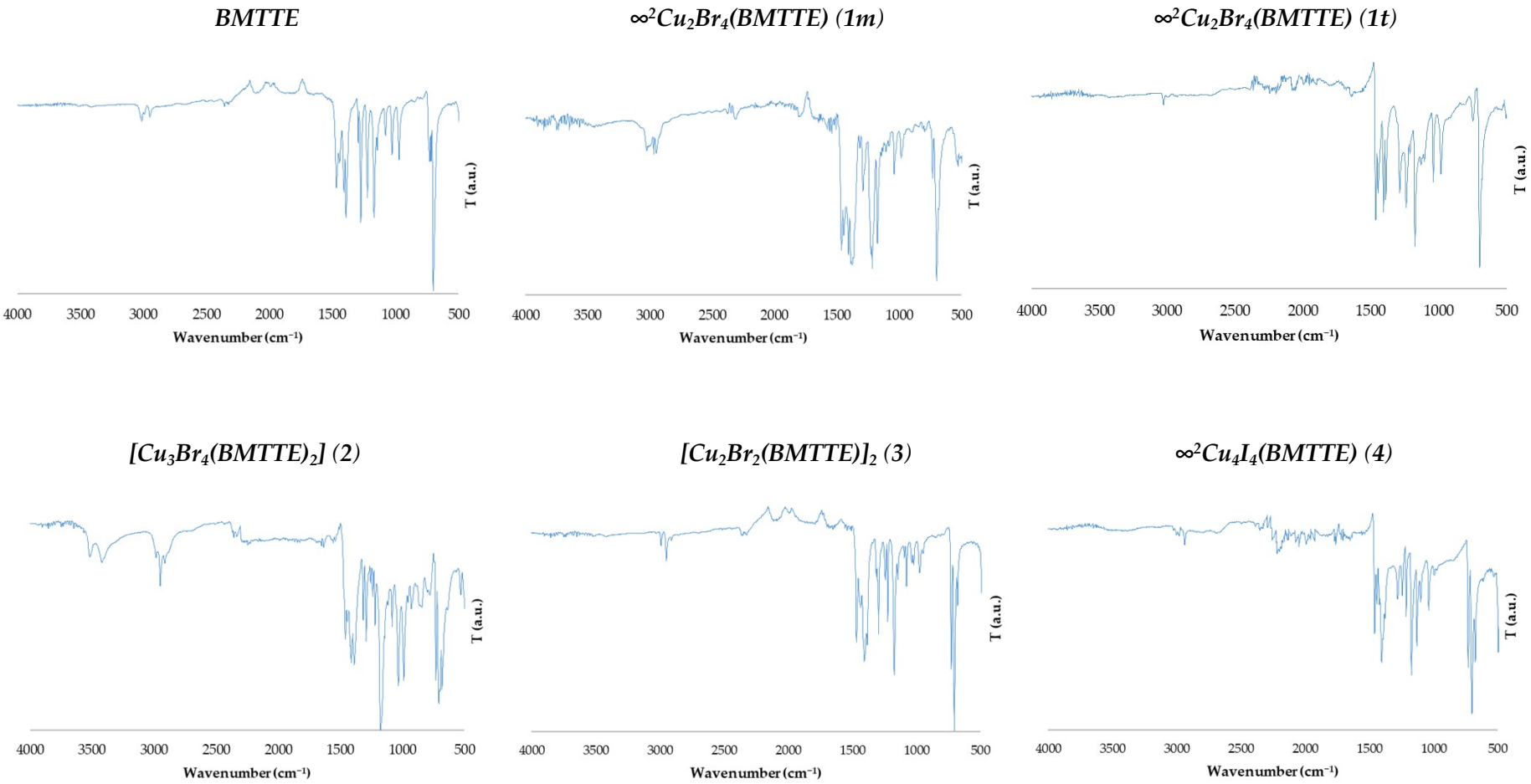

Figure S1: Infrared spectra (IR) of the BMTTE ligand and the complexes **1-4**.

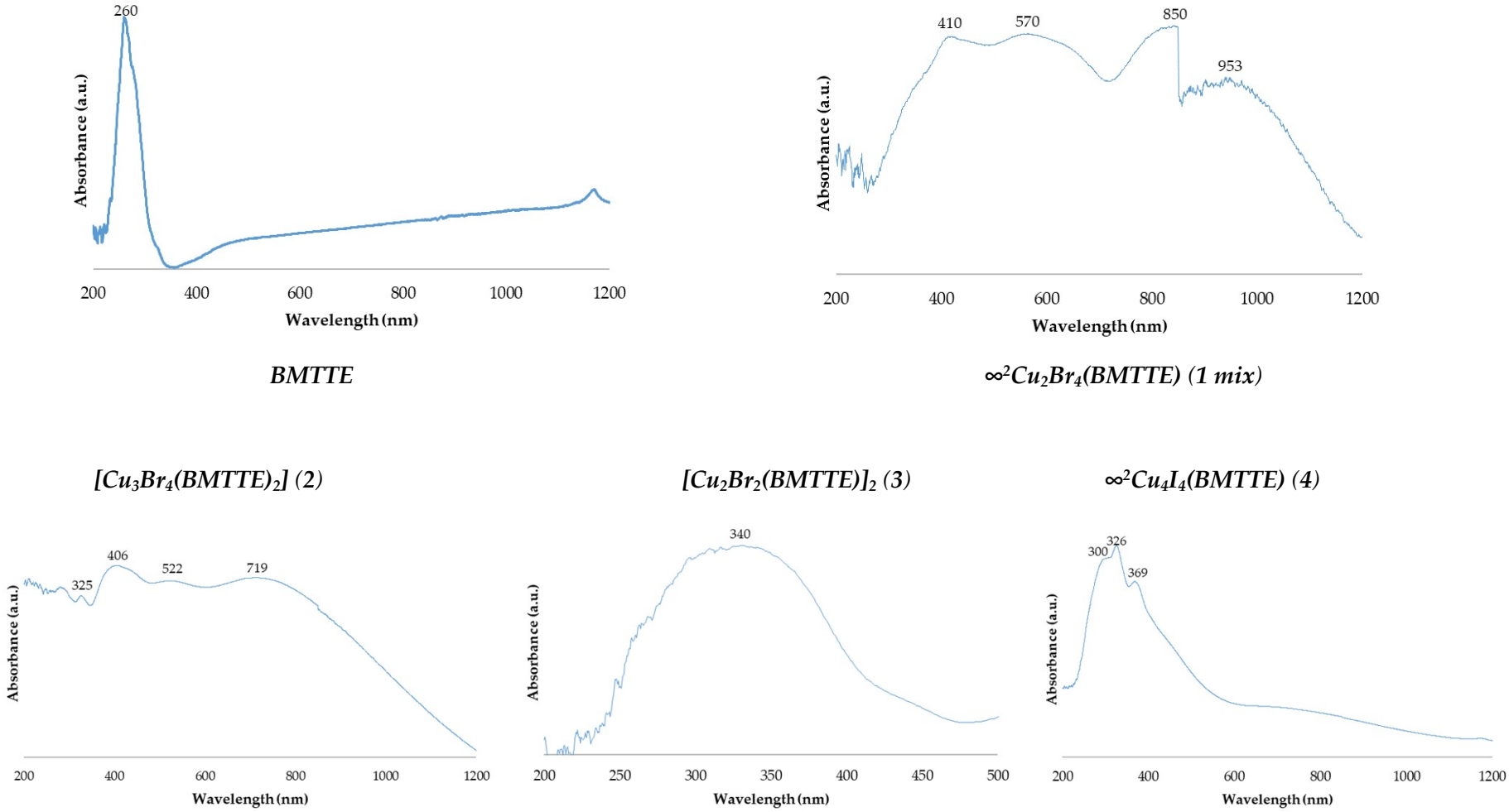

Figure S2: UV-Vis spectra of the BMTTE ligand and the complexes **1-4**.

Method A (1)

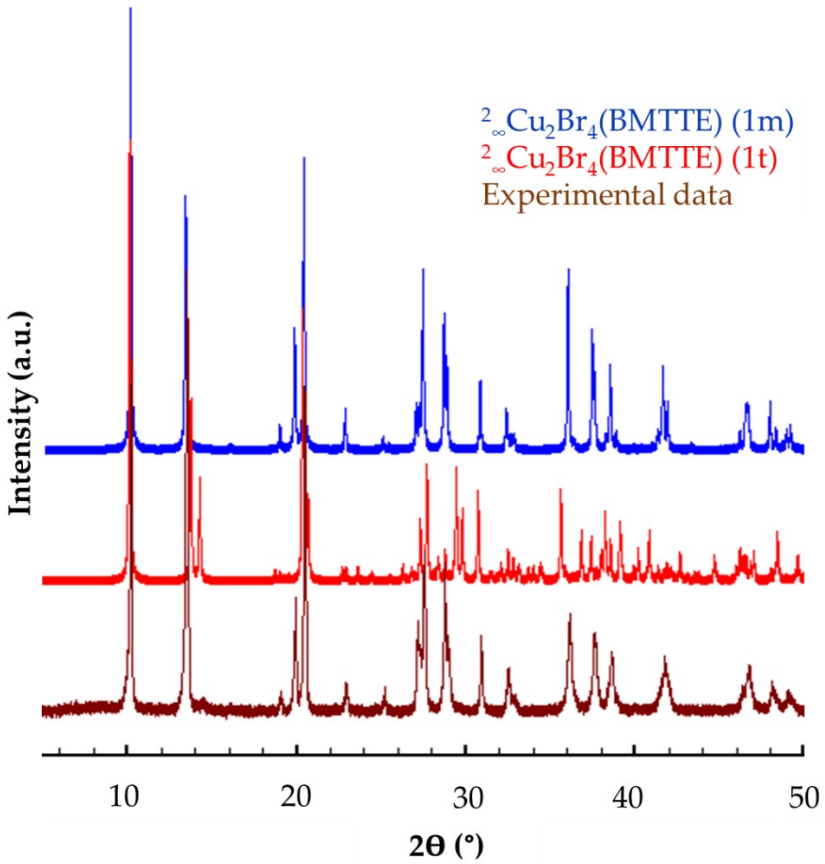

Method B (1)

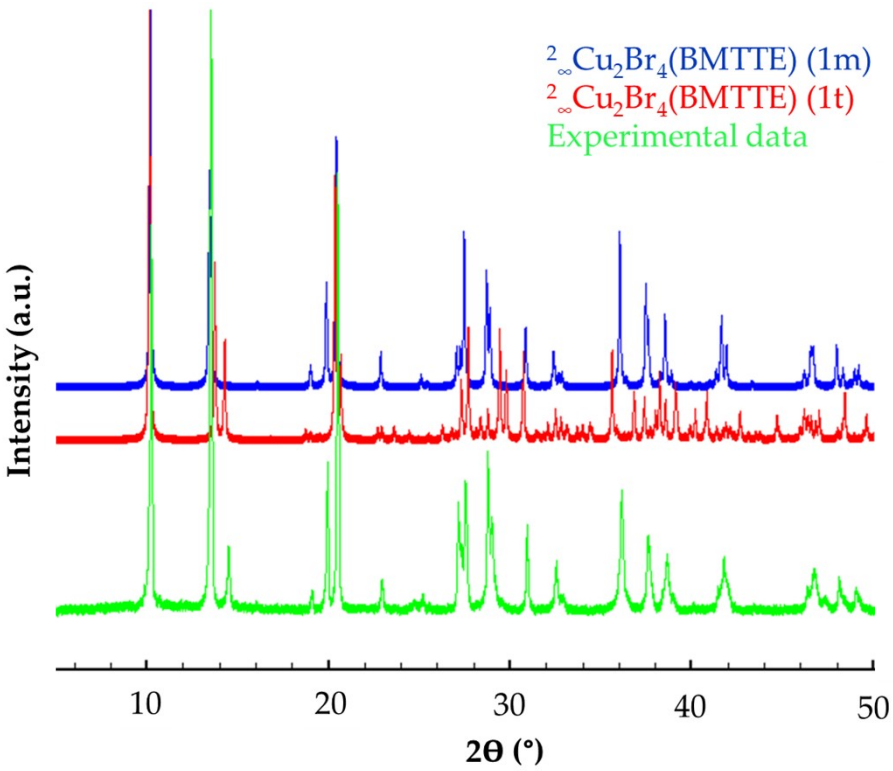

Figure S3: Powder X-ray diffraction (PXRD) comparison between bulk experimental data and simulation based on single crystal X-ray diffraction of **1**

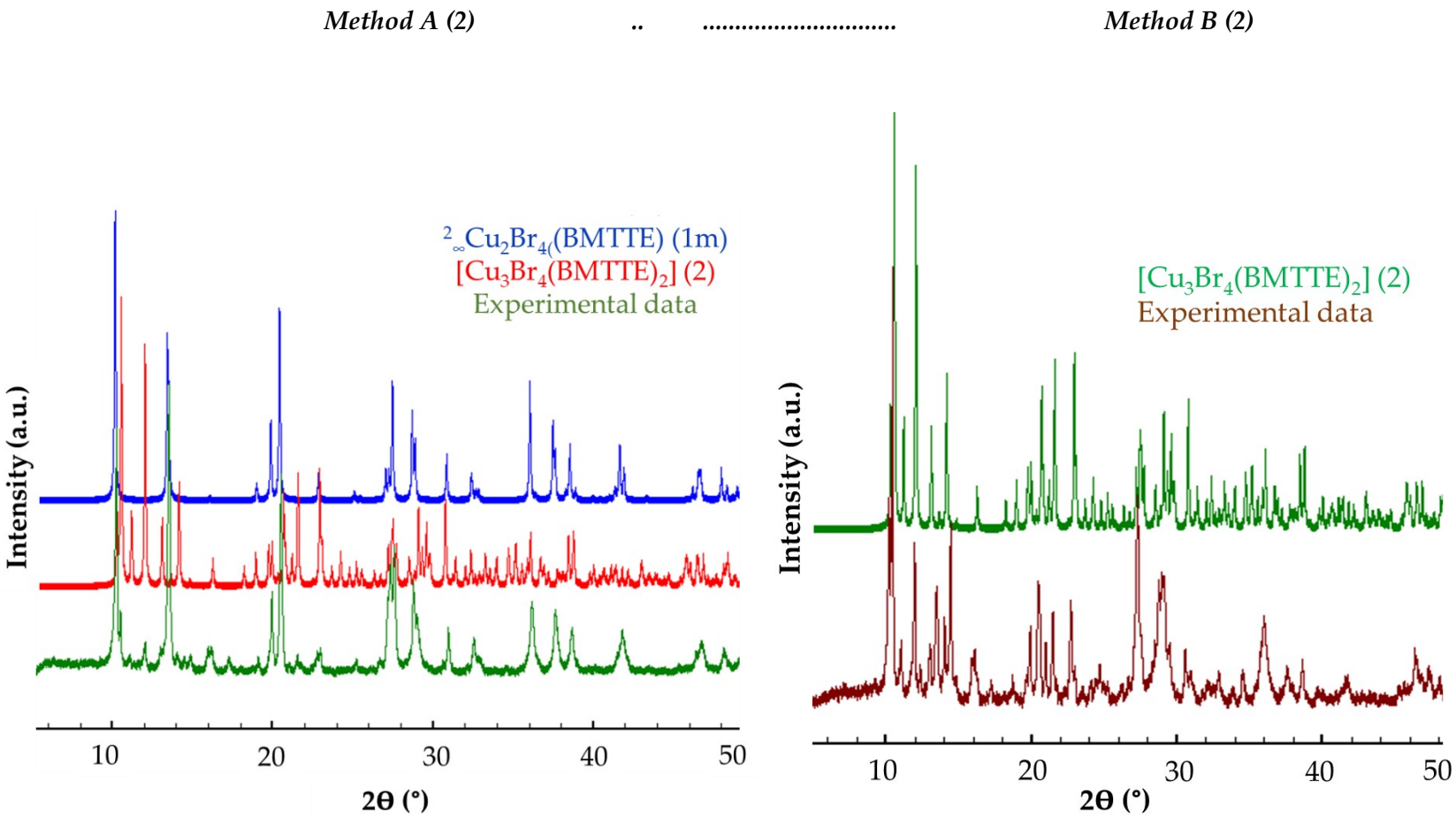

Figure S4: Powder X-ray diffraction (PXRD) comparison between bulk experimental data and simulation based on single crystal X-ray diffraction of **2.**

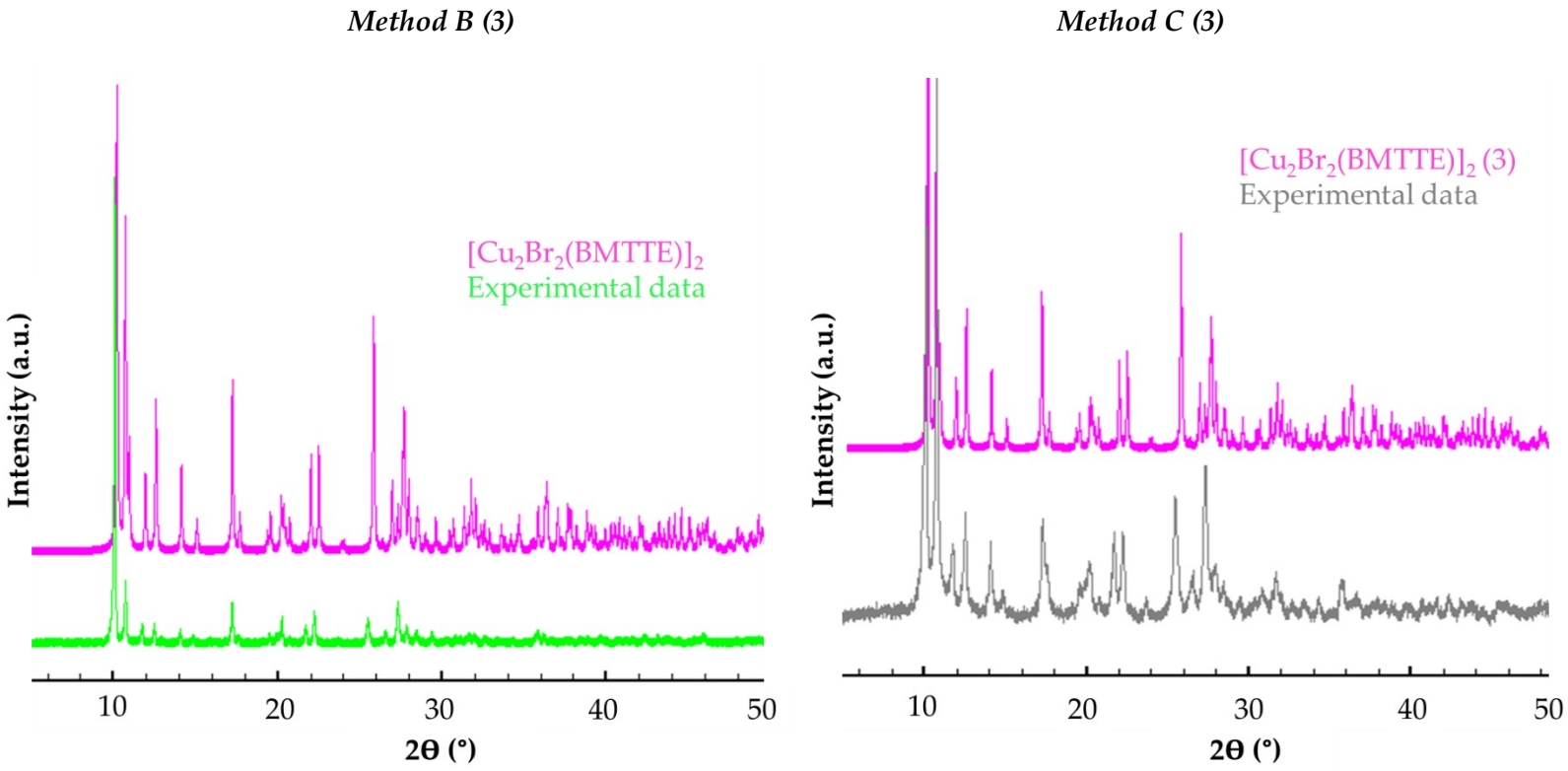

Figure S5: Powder X-ray diffraction (PXRD) comparison between bulk experimental data and simulation based on single crystal X-ray diffraction of **3.**

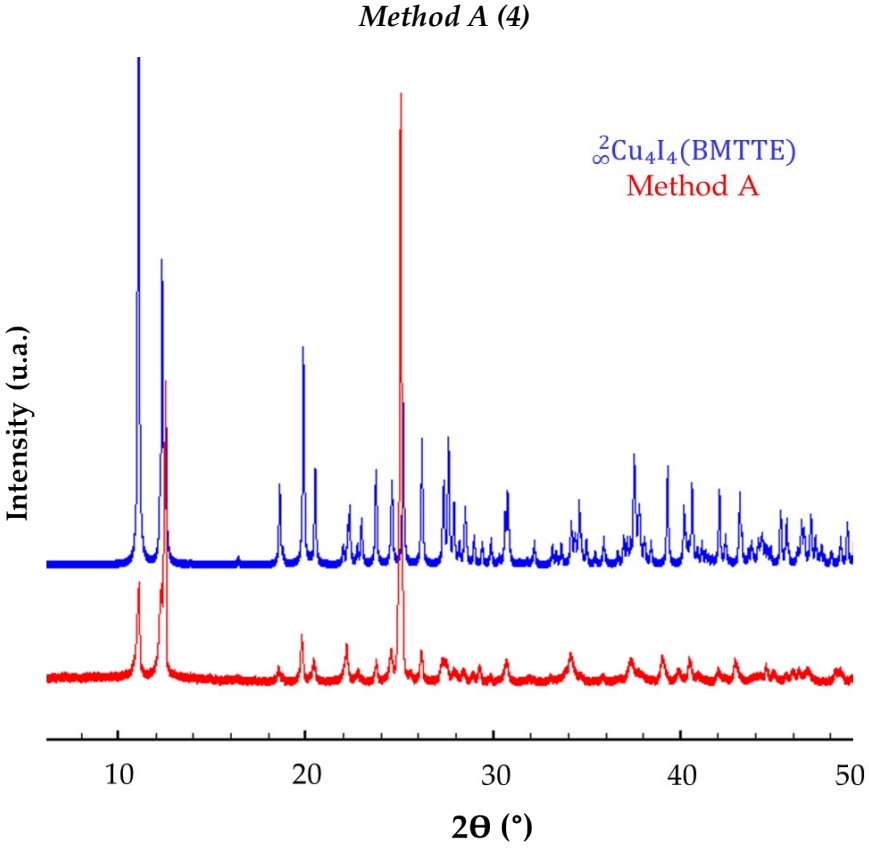

Figure S6: Powder X-ray diffraction (PXRD) comparison between bulk experimental data and simulation based on single crystal X-ray diffraction of **4.**

2. Crystallography

Table S1: Crystal data and structure refinement

Compound		1m	1t	2	3	4
Empirical formula		$C_3H_5Br_2CuN_4S$	$C_6H_{10}Br_4Cu_2N_8S_2$	$C_{12}H_{20}Br_4Cu_3N_{16}S_4$	$C_{12}H_{20}Br_4Cu_4N_{16}S_4$	$C_3H_5Cu_2I_2N_4S_2$
Formula weight		352.53	705.06	1026.94	1090.48	510.05
Crystal system, space group		Monoclinic, *C2/m*	Triclinic, *P-1*	Monoclinic, $P2_1/n$	Monoclinic, $P2_1/n$	Triclinic, *P-1*
CCDC reference		2264490	2264491	2264492	2264493	2264494
Unit cell dimensions	**a/Å**	14.182(2)	6.9967(5)	9.0902(7)	10.2919(10)	7.9700(4)
	b/Å	6.9954(10)	9.1986(8)	10.2268(7)	9.6293(9)	8.3490(5)
	c/Å	9.3508(14)	13.6109(11)	15.9673(11)	14.8207(13)	8.9632(5)
	α/°	-	71.516(3)	-	-	111.095(2)
	β/°	111.712(4)	86.140(2)	98.710(2)	92.996(3)	98.825(2)
	γ/°	-	87.700(2)	-	-	107.631(2)
Volume/A^3		861.9(2)	828.76(12)	1467.26(18)	1466.8(2)	506.69(5)
Z, ϱ_{calc}/g·cm^{-3}		4/2.717	2/2.825	2/2.324	2/2.469	2/3.343
F(000)		664	664	990	1048	462
Crystal size (mm^3)		0.069x0.063x0.019	0.123x0.074x0.015	0.153x0.125x0.098	0.255x0.144x0.093	0.098x0.056x0.035
Abs. coeff. (mm^{-1})		16.246	12.466	7.924	8.633	10.447
θ Range (°)		5.091-71.873	2.371-28.343	2.373-28.352	2.752-28.378	2.549 – 28.379
Max./min. transmission		0.7535/0.4461	0.7461/0.6127	0.7457/0.5666	0.7457/0.2994	0.7457 / 0.5671
Reflections collected		8529	28424	19153	22985	20806
Independent reflections (R_{int})		923 (0.0504)	4130 (0.0407)	3662 (0.0425)	3634 (0.1336)	2534 (0.0245)
Final R indices [I>2σ(I)]		R1 =0.0229; wR2=0.0633	R1 = 0.0219;;wR2 = 0.0500	R1 = 0.0275wR2 = 0.0549	R1 = 0.0453wR2 = 0.1047	R1 = 0.0178, wR2 = 0.037

Table S2: Selected bond lengths/Å and angles/° for **1m** and **1t**

	1m	**1t**		**1m**	**1t**		**1t**
Br1-Cu1	2.4381(5)	2.4434(4)	**Cu2-Br3-Cu1**		94.075(12)	**N3-Cu1-Br2**	99.22(5)
Br1-Cu1#1	2.4420(5)		**Cu2-Br4-Cu1#1**		94.313(13)	**N3-Cu1-Br3**	96.83(5)
Br2-Cu1		2.4396(3)	**Br1-Cu1-Br1#2**	164.44(2)		**N3-Cu1-Br4#2**	100.09(5)
Br3-Cu1		2.4366(4)	**Br1-Cu1-Br1#1**	86.330(15)		**Br2-Cu2-Br1#1**	162.965(14)
Br4-Cu1#1		2.4389(3)	**Br1#2-Cu1-Br1#1**	91.55(2)		**Br3-Cu2-Br1#1**	90.780(13)
Br1-Cu2#2		2.4500(4)	**Br2-Cu1-Br1**		164.460(14)	**Br4-Cu2-Br1#1**	85.939(12)
Br2-Cu2		2.4469(4)	**Br3-Cu1-Br1**		92.456(13)	**Br3-Cu2-Br2**	86.197(12)
Br3-Cu2		2.4283(3)	**Br4#2-Cu1-Br1**		85.961(12)	**Br4-Cu2-Br2**	92.419(13)
Br4-Cu2		2.4332(3)	**Br3-Cu1-Br2**		86.177(12)	**Br3-Cu2-Br4**	164.175(14)
Cu1-N3	2.223(3)	2.2441(18)	**Br4#2-Cu1-Br2**		90.853(12)	**N7-Cu2-Br4**	96.64(5)
Cu2-N7		2.2307(19)	**Br3-Cu1-Br4#2**		163.077(14)	**N7-Cu2-Br3**	99.18(5)
Cu1-Br1-Cu1#1	93.671(15)		**N3-Cu1-Br1#1**	96.27(6)		**N7-Cu2-Br2**	96.21(5)
Cu1-Br1-Cu2#2		93.776(13)	**N3-Cu1-Br1**	99.29(6)	96.31(5)	**N7-Cu2-Br1#1**	100.83(5)
Cu1-Br2-Cu2		93.534(12)	Symmetry code: (**1m**) #1 -x+3/2,-y+3/2,-z; #2 -x+3/2,y-1/2,-z; (**1t**) #1 x-1,y,z; #2 x+1,y,z;				

Table S3: Selected bond lengths/Å and angles/° for **2** and **3**

	2	**3**		**2**	**3**		**2**	**3**
Cu1-Br1	2.6349(4)	2.5400(5)	**N4-Cu1-Br1**	87.02(6)	99.75(7)	**N3-Cu2-N3#1**	180.0	
Cu1-Br2	2.4077(5)		**N4-Cu1-Br2**	98.39(7)		**N3-Cu2-Br1#1**	93.33(7)	96.34(8)
Br2-Cu1#1		2.5845(5)	**N4-Cu1-Br2#1**		113.54(7)	**N3#1-Cu2-Br1#1**	86.66(7)	
Cu1-N4	2.081(3)	2.035(3)	**N4-Cu1-Cu2#1**		99.47(7)	**N3-Cu2-Br2**	86.14(7)	130.85(9)
Cu1-N8	1.955(2)	2.026(3)	**N8-Cu1-N4**	130.34(10)		**N3#1-Cu2-Br2**	93.86(7)	
Cu2-Br1	2.4247(3)	2.5264(6)	**N8-Cu1-Br1**	108.68(7)	104.27(8)	**N3-Cu2-Cu2#1**		102.57(9)
Br1-Cu2#1		2.5952(5)	**N8-Cu1-Br2**	122.56(7)		**N3-Cu2-Cu1#1**		147.14(8)
Br2-Cu2	3.0865(3)	2.3881(5)	**N8-Cu1-Br2#1**		95.60(8)	**Br1#1-Cu2-Cu2#1**		57.729(17)
Cu2-Cu1#1		2.8551(6)	**N8-Cu1-Cu2#1**		124.57(9)	**Br1-Cu2-Cu2#1**		60.291(18)
Cu2-Cu2#1		2.6376(9)	**N8-Cu1-N4**		135.96(11)	**Br1#1-Cu2-Cu1#1**		55.307(13)
Cu2-N3	2.037(2)	2.035(3)	**Br1#1-Cu2-Br1**	179.999(12)	118.020(19)	**Br1-Cu2-Cu1#1**		110.95(2)
Br2-Cu1-Br1	101.147(16)		**Br1-Cu2-Br2**	89.184(9)	107.245(19)	**Br2-Cu2-Cu2#1**		126.58(3)
Br1-Cu1-Br2#1		104.275(18)	**Br1#1-Cu2-Br2**	90.816(9)	108.489(18)	**Br2-Cu2-Cu1#1**		58.254(13)
Br1-Cu1-Cu2#1		57.147(13)	**N3-Cu2-Br1**	86.67(7)	96.53(8)	**Cu2#1-Cu2-Cu1#1**		77.43(2)
Br2#1-Cu1-Cu2#1		51.792(13)						

Symmetry code: (**2**) #1 -x+1,-y+2,-z+1; (**3**) #1 -x+1,-y,-z+1;

Table S4: Selected bond lengths/Å and angles/° for **4**

I2-Cu1#1	2.6254(4)	**I2#1-Cu1-I1**	106.416(13)	**I1-Cu2-I1#1**	121.561(13)
I2-Cu1#2	2.6515(4)	**I2-Cu1-Cu2#1**	153.529(16)	**I1#1-Cu2-Cu1#1**	59.131(11)
I2-Cu2	2.6081(4)	**I2#1-Cu1-Cu2#1**	58.241(11)	**I1-Cu2-Cu1#1**	109.944(14)
I1-Cu1	2.6816(4)	**I1-Cu1-Cu2#1**	59.941(11)	**Cu2#1-Cu2-I1**	61.205(13)
I1-Cu2	2.6816(4)	**N3-Cu1-I2#3**	103.24(6)	**Cu2#1-Cu2-I1#1**	60.356(14)
I1-Cu2#1	2.7039(4)	**N3-Cu1-I2#1**	123.99(7)	**Cu2#1-Cu2-Cu1#1**	79.644(17)
Cu2-Cu2#1	2.6291(7)	**N3-Cu1-I1**	96.27(6)	**N4-Cu2-I2**	122.66(6)
Cu1-Cu2#1	2.7305(5)	**N3-Cu1-Cu2#1**	100.90(6)	**N4-Cu2-I1#1**	98.28(7)
Cu1-N3	2.089(2)	**I2-Cu2-I1#1**	109.948(13)	**N4-Cu2-I1**	97.48(6)
Cu2-N4	2.051(2)	**I2-Cu2-I1**	107.410(13)	**N4-Cu2-Cu1#1**	150.82(7)
I2#1-Cu1-I2#3	114.358(13)	**I2-Cu2-Cu1#1**	58.863(11)	**N4-Cu2-Cu2#1**	106.31(7)
I2#1-Cu1-I1	110.112(13)	**I2-Cu2-Cu2#1**	131.00(2)		

Symmetry code: #1 -x+1,-y+2,-z+1; #2 x+1,y,z; #3 x-1,y,z;

Table S5: Main hydrogen bonds (A,°)

	D-H···A	d(D-H)	d(H···A)	d(D···A)	∠(DHA)
1m	**C(12)-H(12A)...Br(1)#1**	0.96	3.11	3.655(3)	117.2
	C(12)-H(12B)...Br(1)#2	0.96	3.12	3.994(4)	152.4
1t	**C(22)-H(22A)...Br(3)#2**	0.98	2.98	3.737(2)	134.5
	C(22)-H(22A)...N(4)#2	0.98	2.68	3.455(3)	136.7
	C(22)-H(22C)...N(6)#3	0.98	2.62	3.597(3)	176.0
	C(12)-H(12A)...N(2)#4	0.98	2.68	3.656(3)	171.4
	C(12)-H(12C)...Br(2)#5	0.98	3.05	3.868(2)	141.3
	C(2)-H(2B)...C(12)#1	0.99	2.82	3.653(3)	142.7
2	**C(12)-H(12B)...N(7)#1**	0.98	2.69	3.528(4)	143.4
	C(22)-H(22C)...Br(2)#2	0.98	2.90	3.506(3)	121.1
	C(22)-H(22B)...Br(2)#3	0.98	2.82	3.578(3)	135.0
	C(2)-H(2B)...Br(2)#2	0.99	3.12	3.844(3)	130.8
	C(2)-H(2B)...Br(1)#4	0.99	2.84	3.704(3)	146.2
	C(1)-H(1B)...Br(1)#2	0.99	3.11	3.663(3)	116.6
3	**C(22)-H(22A)...S(1)#2**	0.98	2.98	3.686(2)	130.3
	C(22)-H(22C)...Br(2)#3	0.98	3.01	3.525(2)	113.7
	C(12)-H(12A)...N(2)#4	0.98	2.69	3.608(3)	156.8
	C(1)-H(1B)...N(7)#5	0.99	2.66	3.465(3)	138.2
	C(2)-H(2A)...Br(1)#6	0.99	2.91	3.807(2)	151.4
	C(2)-H(2A)...Br(2)#6	0.99	3.02	3.654(2)	123.0
	C(2)-H(2B)...Br(2)#1	0.99	2.98	3.904(2)	156.0
4	**C(1)-H(1A)...I(2)**	0.99	3.19	3.962(3)	135.6
	C(1)-H(1B)...N(2)#1	0.99	2.62	3.460(3)	142.9
	C(12)-H(12B)...I(2)#2	0.98	3.26	3.999(3)	133.9
	C(12)-H(12C)...I(13)#2	0.98	3.11	3.963(3)	146.4

Symmetry code: (**1m**) #1 -x+2,-y+1,-z+1; #2 x,-y+1,z+1; (**1t**) #1 x-1,y-1,z; #2 x,y-1,z; #3 -x+1,-y,-z+1; #4 -x+2,-y+2,-z;#5 x,y+1,z; (**2**)#1 x-1,y,z;#2 x,y-1,z;#3 -x+3/2,y-1/2,-z+1/2; #4 –x+1/2,y-1/2,-z+1/2; (**3**) #1 -x+1,-y,-z+1; #2 -x+3/2,y+1/2,-z+3/2; #3 x-1/2,-y+1/2,z+1/2; #4 -x+2,-y,-z+1; #5 -x+1,-y+1,-z+1; #6 x+1/2,-y+1/2,z+1/2; (4) #1 x+1,y,z; #2 x-1,y-1,z-1;

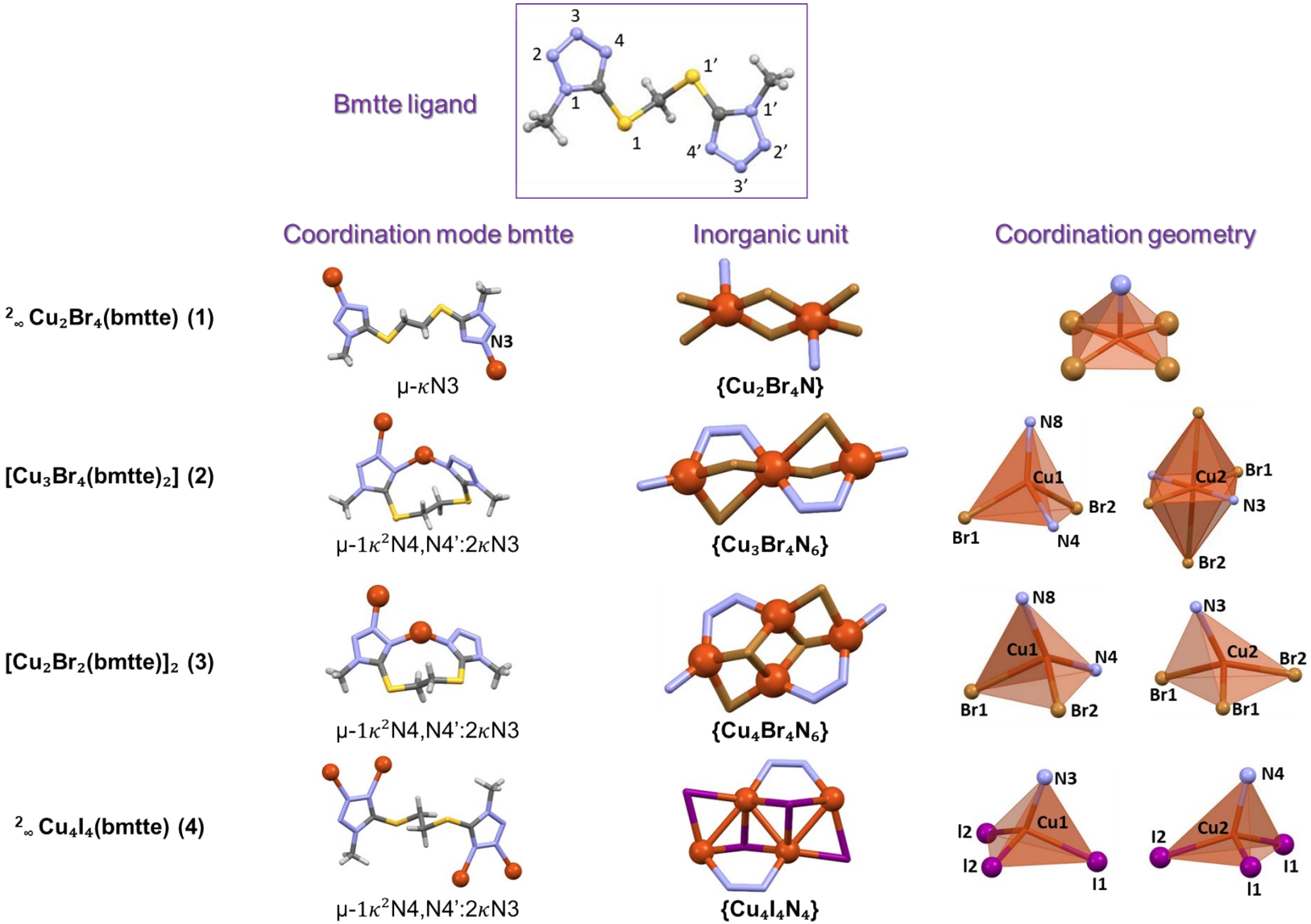

Figure S7: Top: free bmtte ligand. Down: Main structural features of compounds **1-4**

3. Hirshfeld surface analysis

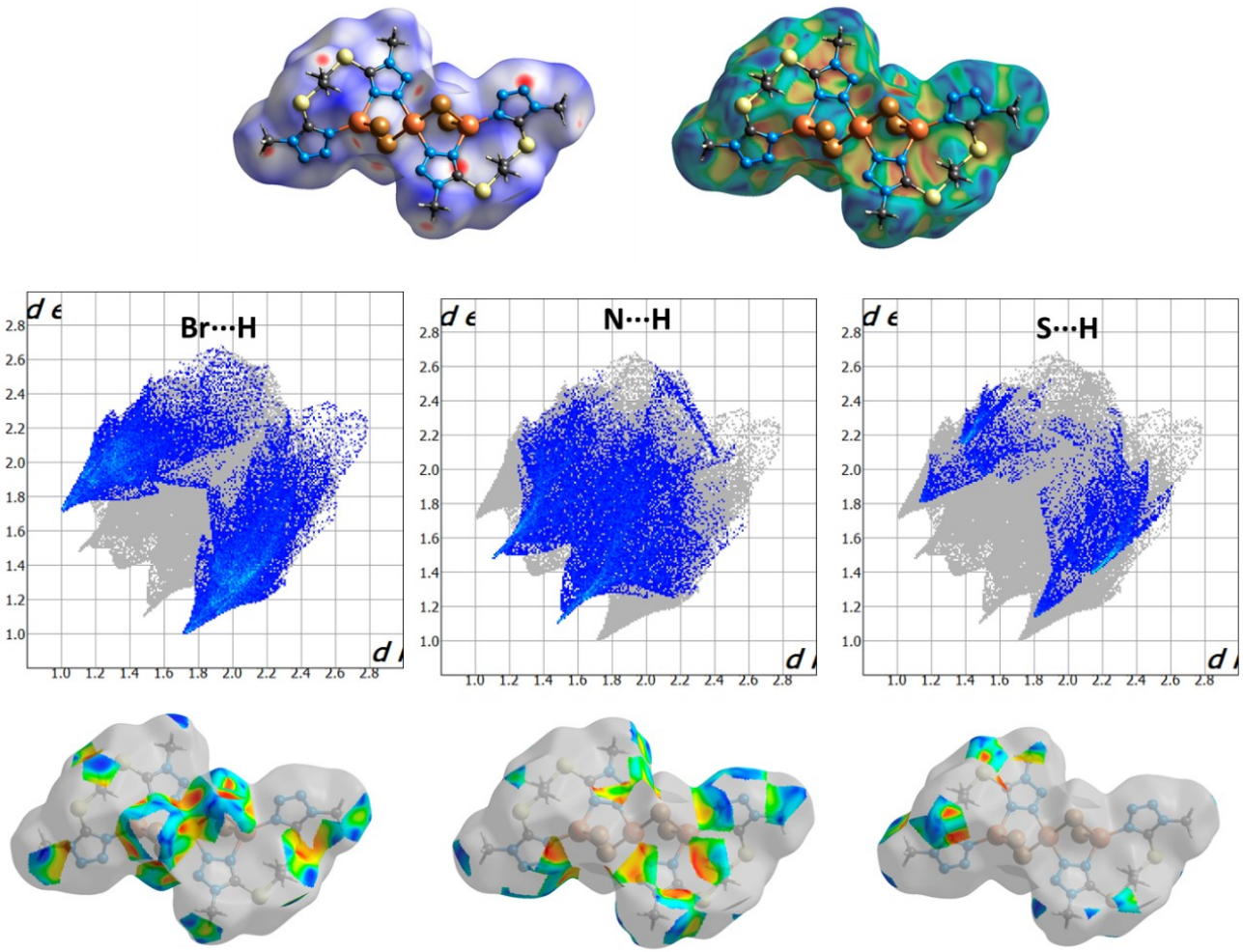

Figure S8: View of the three-dimensional Hirshfeld surface mapped over d_{norm} for (**2**) (top) and Hirshfeld surface mapped with the shape-index property illustrating contacts Br···H, N···H, ·and·S···H in the crystal of (**2**) (down) ; Fingerprint plots into H···Br/ Br···H, H···N/ N···H, S···H/ H···S contacts

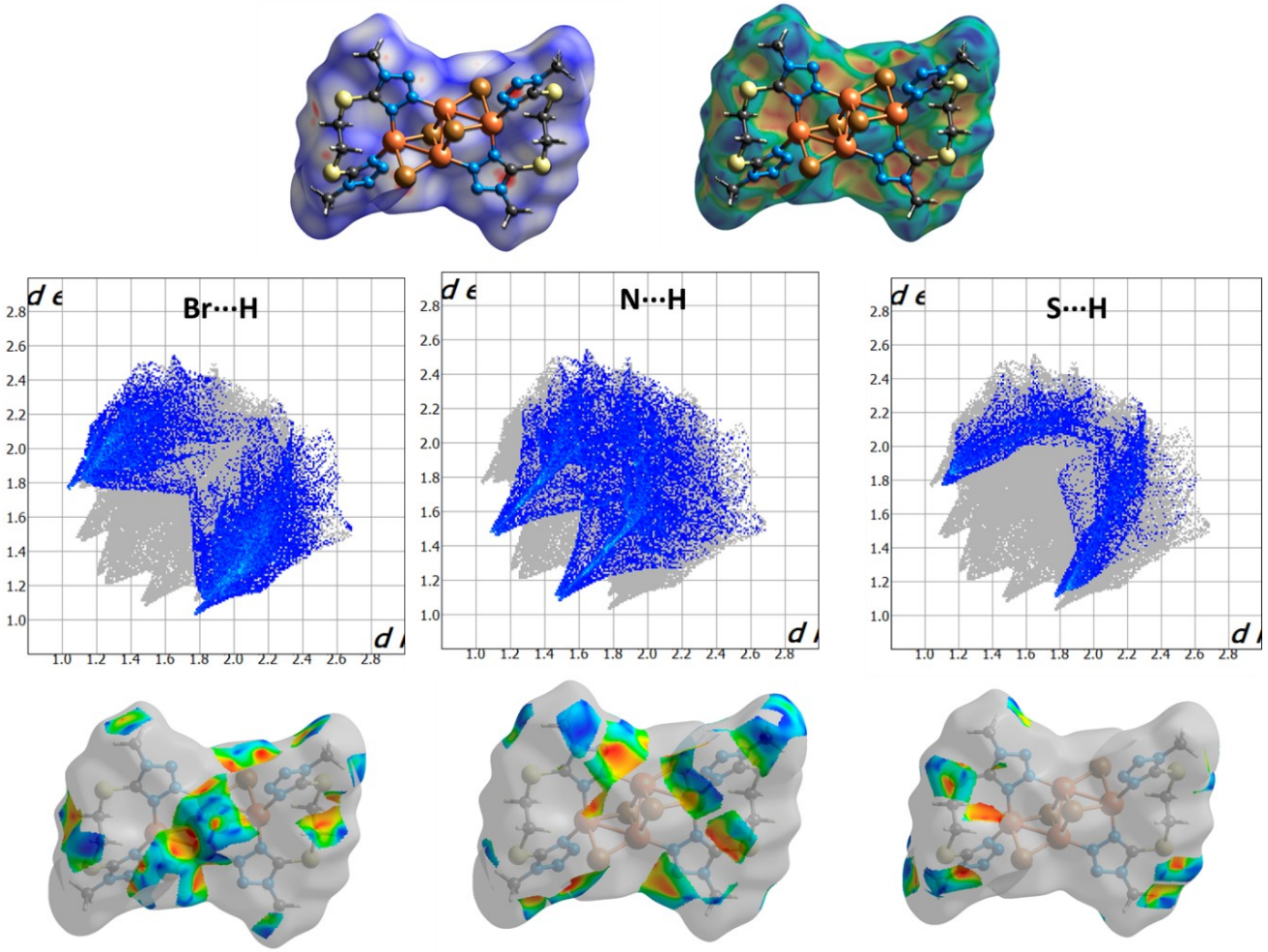

Figure S9: View of the three-dimensional Hirshfeld surface mapped over d_{norm} for (**3**) (top) and Hirshfeld surface mapped with the shape-index property illustrating contacts Br···H, N···H, ·and·S···H in the crystal of (**3**) (down). Fingerprint plots into H···Br/ Br···H, H···N/ N···H, S···H/ H···S contacts.

4. Thermal stability

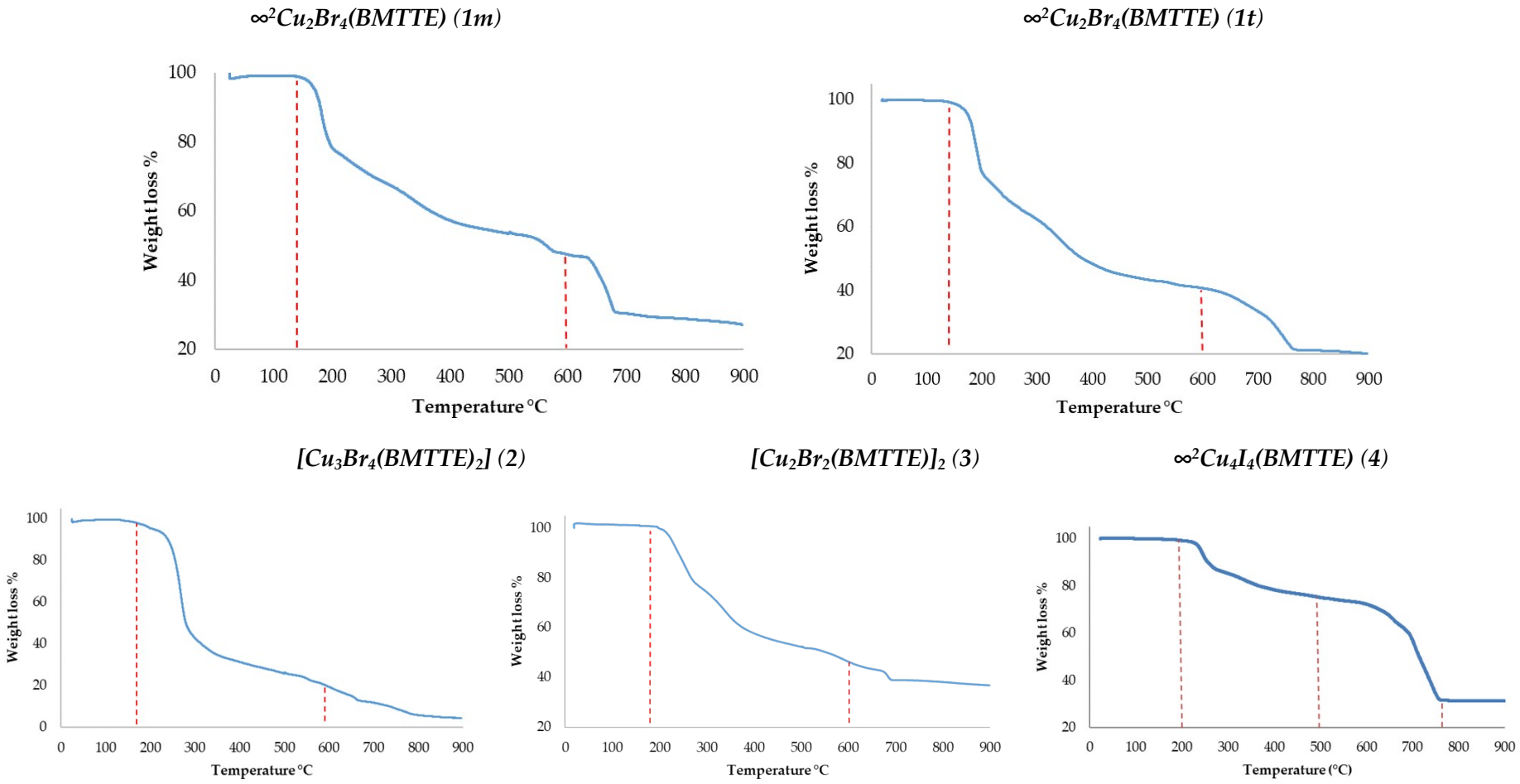

Figure S10: Thermogravimetric analysis (TGA)

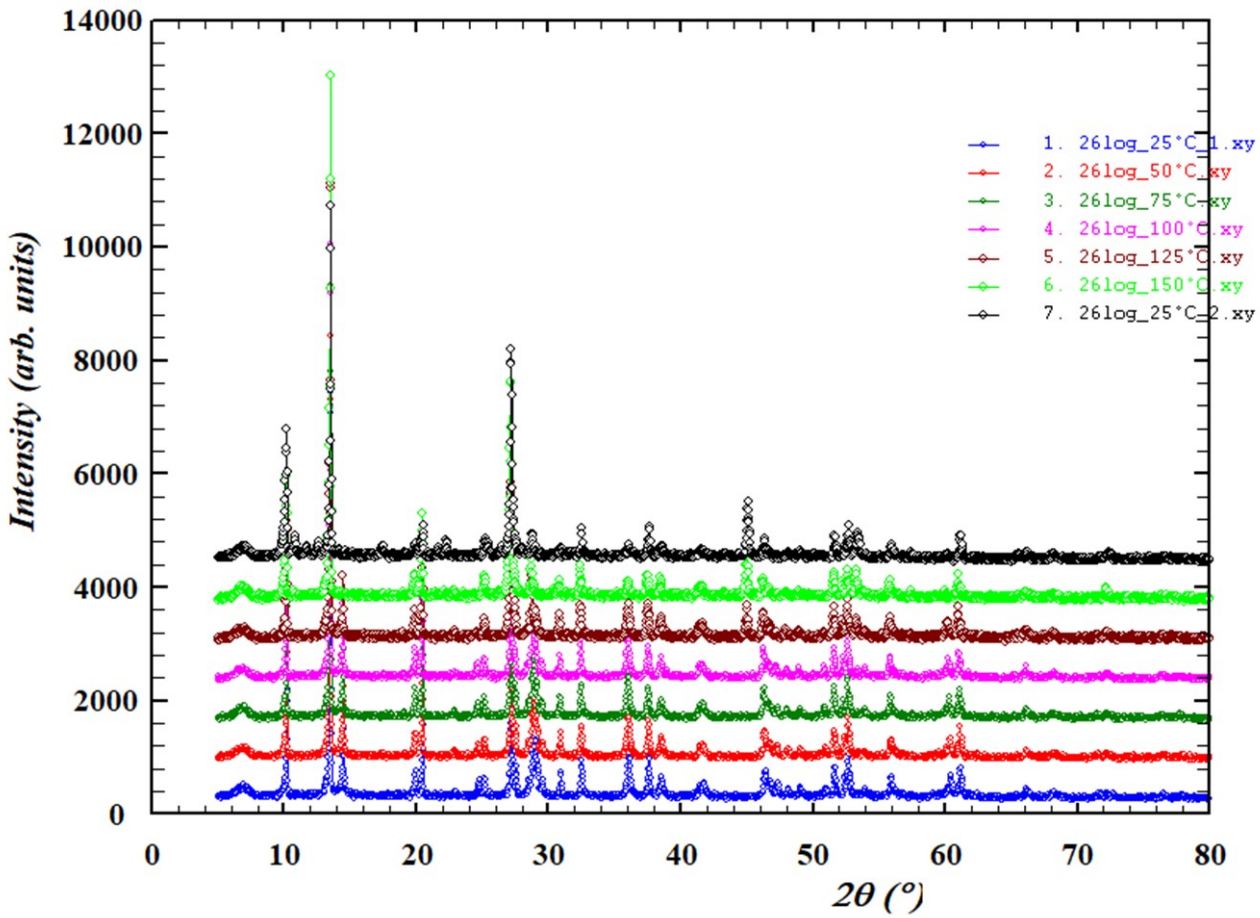

Figure S11: Variable-temperature X-ray powder diffraction of **1m** (blue) in the range 25 –150ºC with XRD pattern of the final product at room temperature after heating.

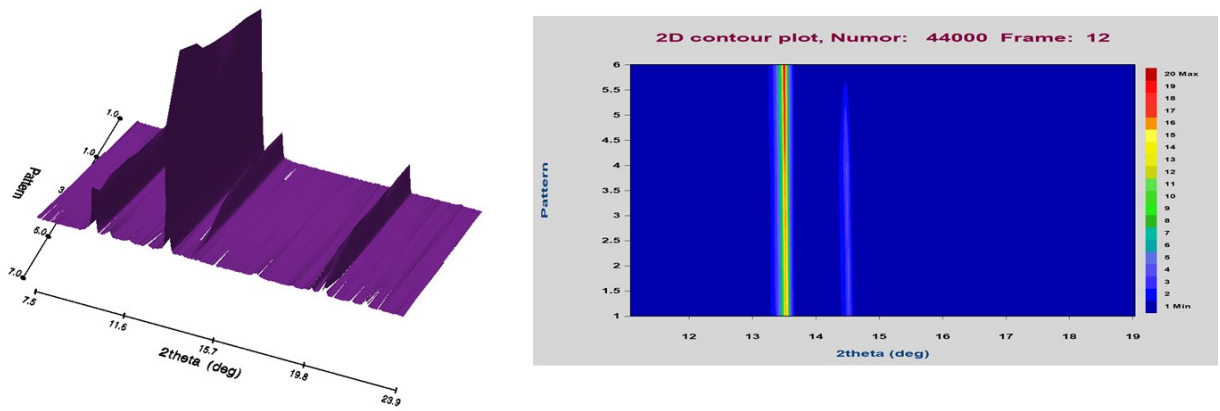

Figure S12:. Three (left) and Two-dimensional (right) intensity contours of **1m** extracted from the XRTD patterns collected as a function of the temperature in the range 25–150°C.

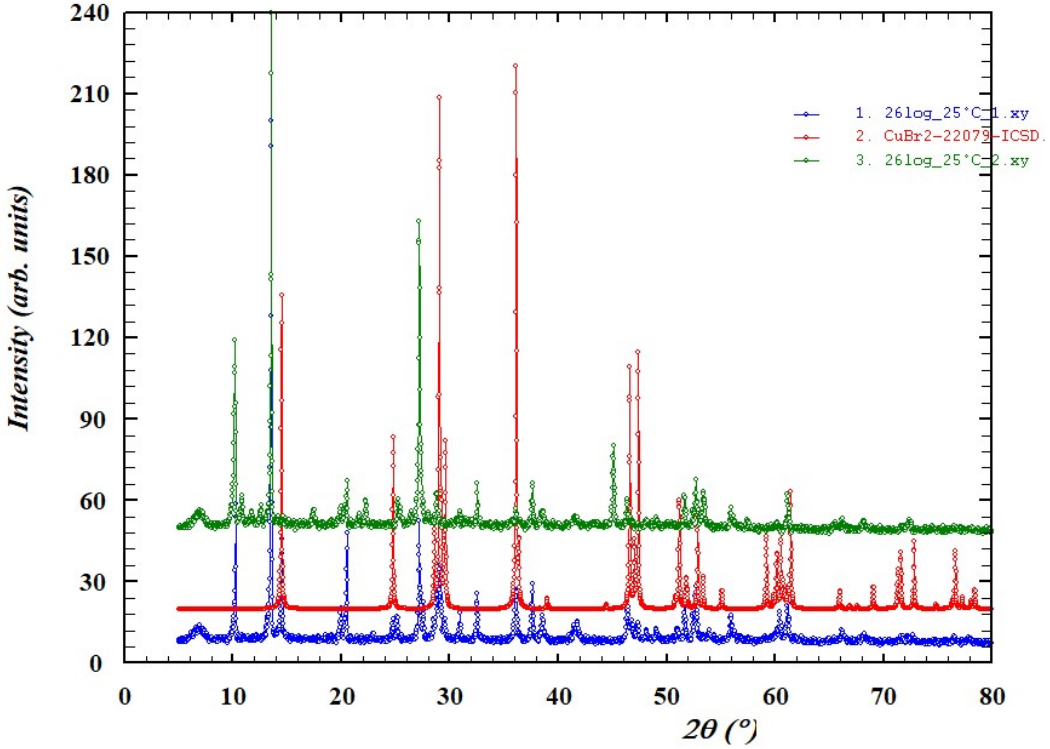

Figure S13: 1m before (blue) and after (green) heat treatment with the XRD pattern of the $CuBr_2$ metal salt (red).

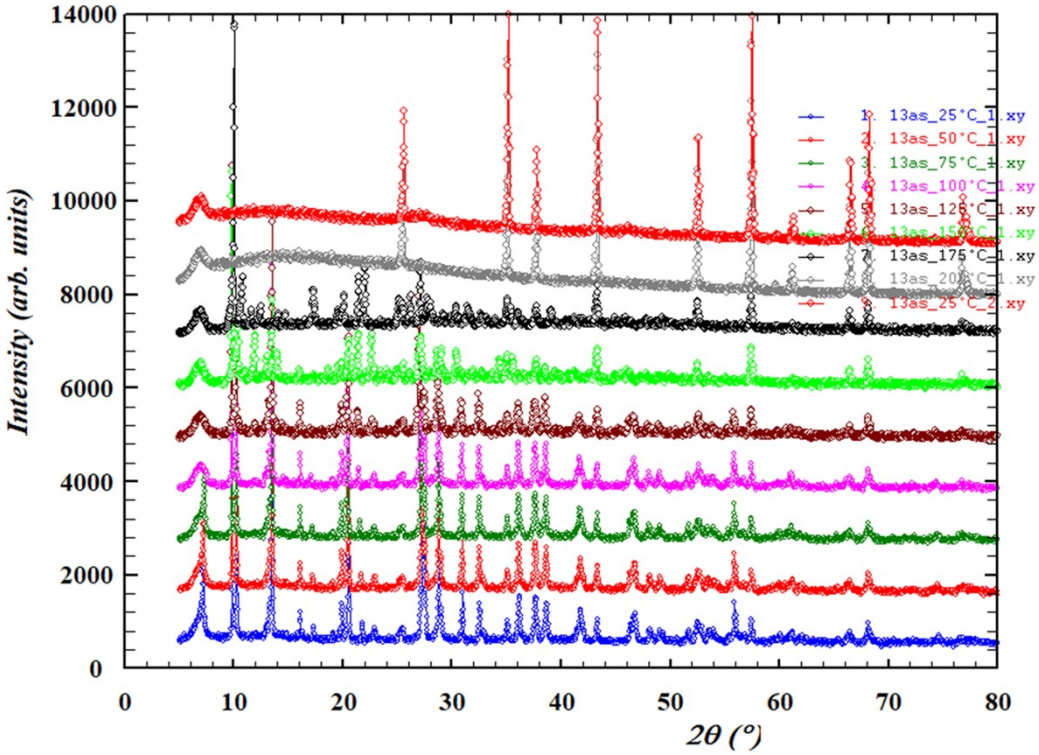

Figure S14 Variable-temperature X-ray powder diffraction of **1m** and **1t** in the range 25 –200ºC with the thermal decomposition after 175 ºC. The remaining peaks are due to the alumina used as a holder.

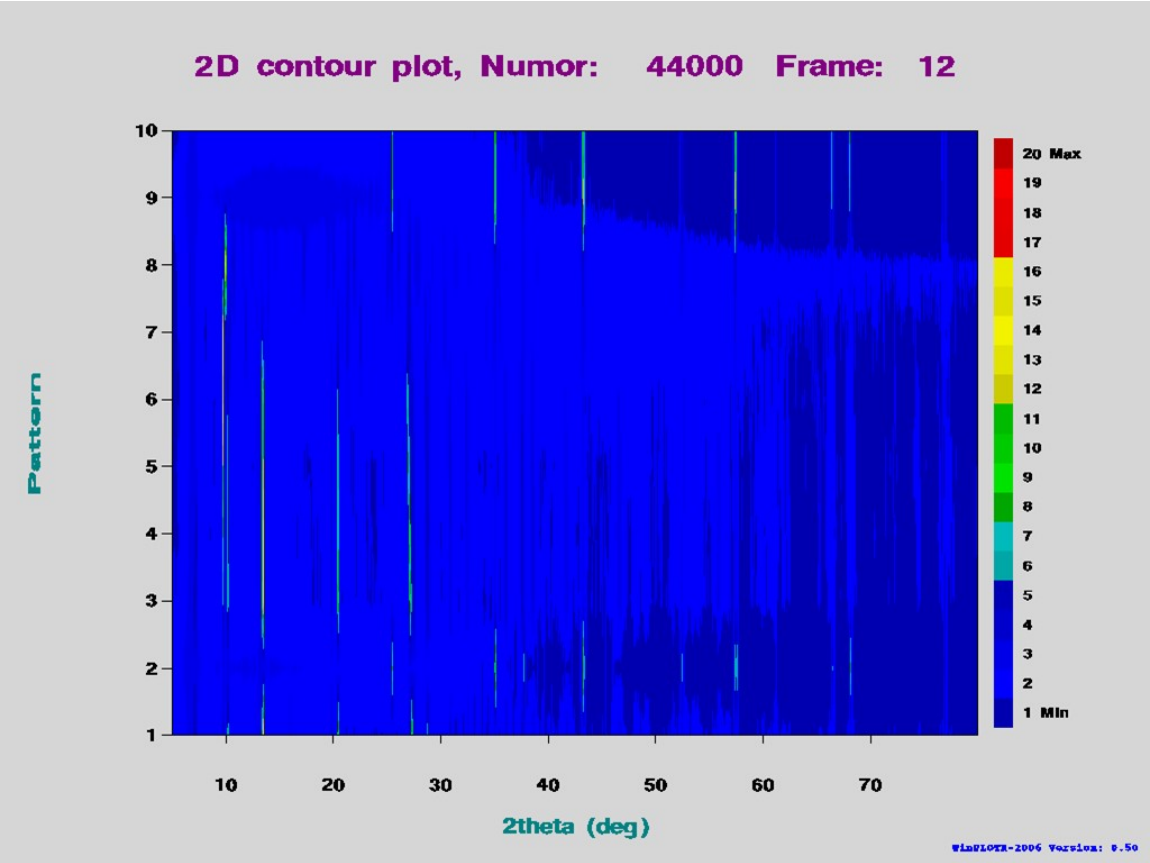

Figure S15: Two-dimensional intensity contours extracted from the XRTD patterns of **1m** and **1t** collected as a function of the temperature range 25–150°C.

5. Water Stability

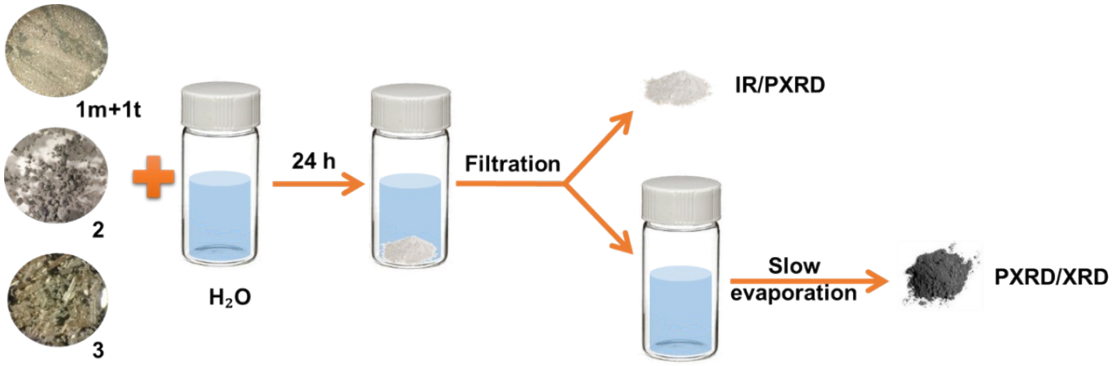

Scheme S1: Experimental process to study the water stability of the compounds.

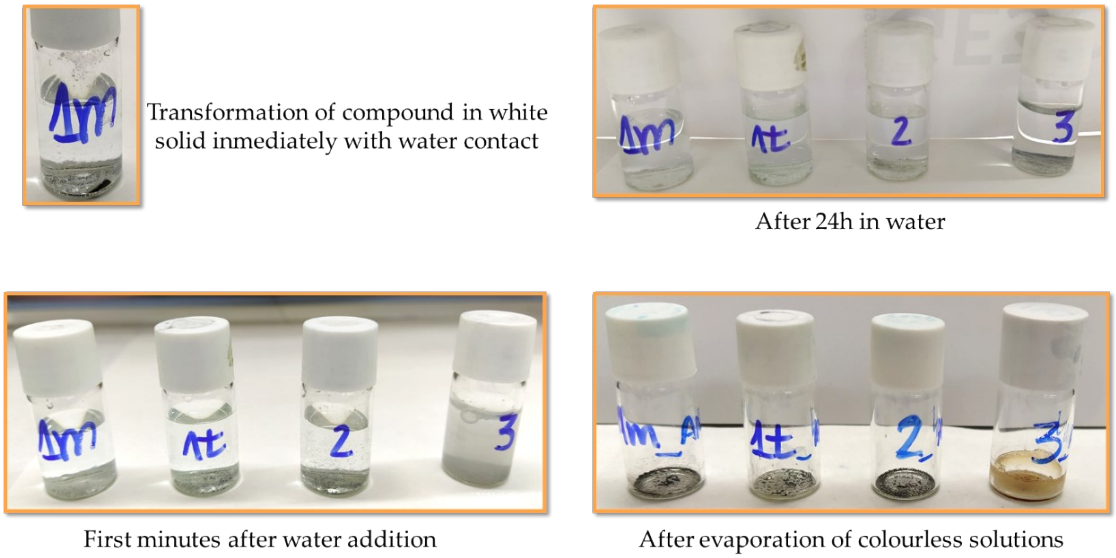

Figure S16: Images of water stability study

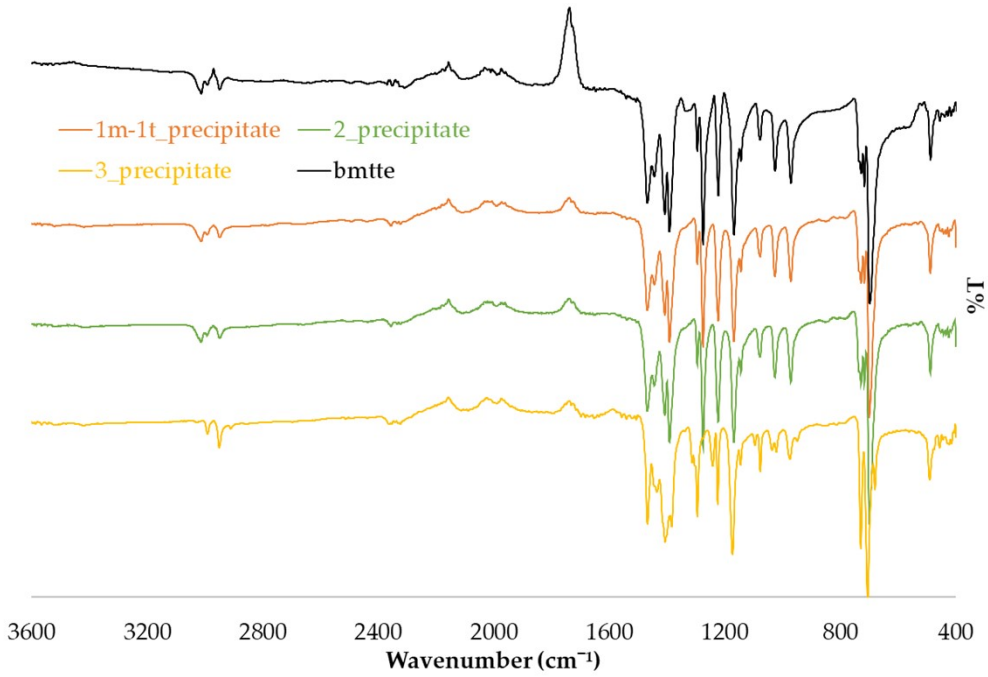

Figure S17: IR of each precipitate **1m-1t**, **2** and **3** after exposure to the water together with IR of bmtte.

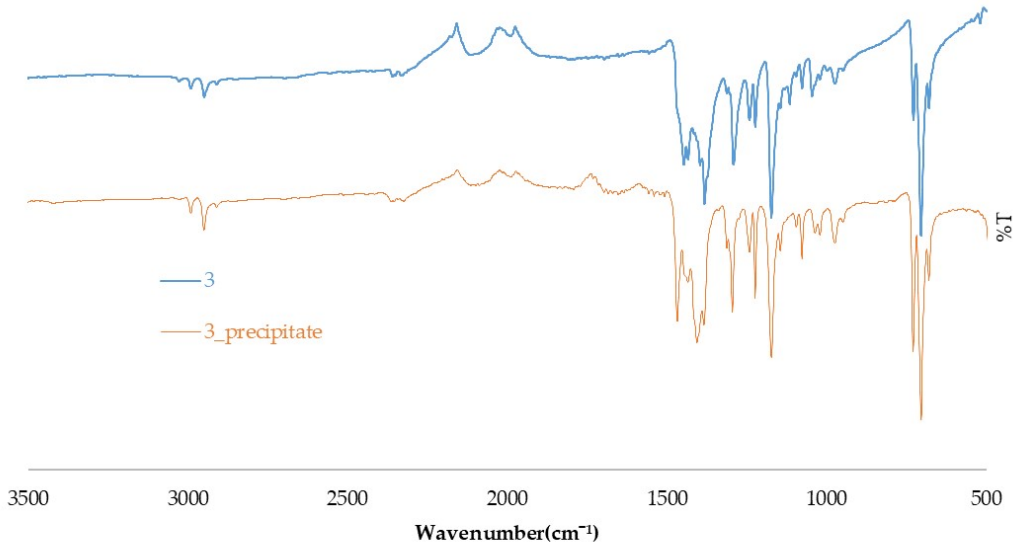

Figure S18: IR comparative of pristine **3** and precipitate after water exposure

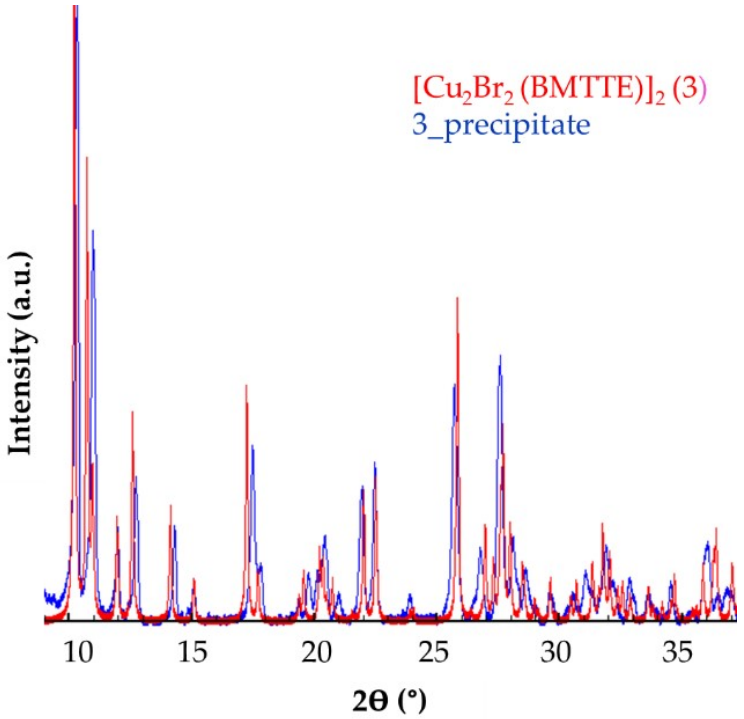

Figure S19: PXRD of **3** after water treatment compared with theoretical patterns of **3**

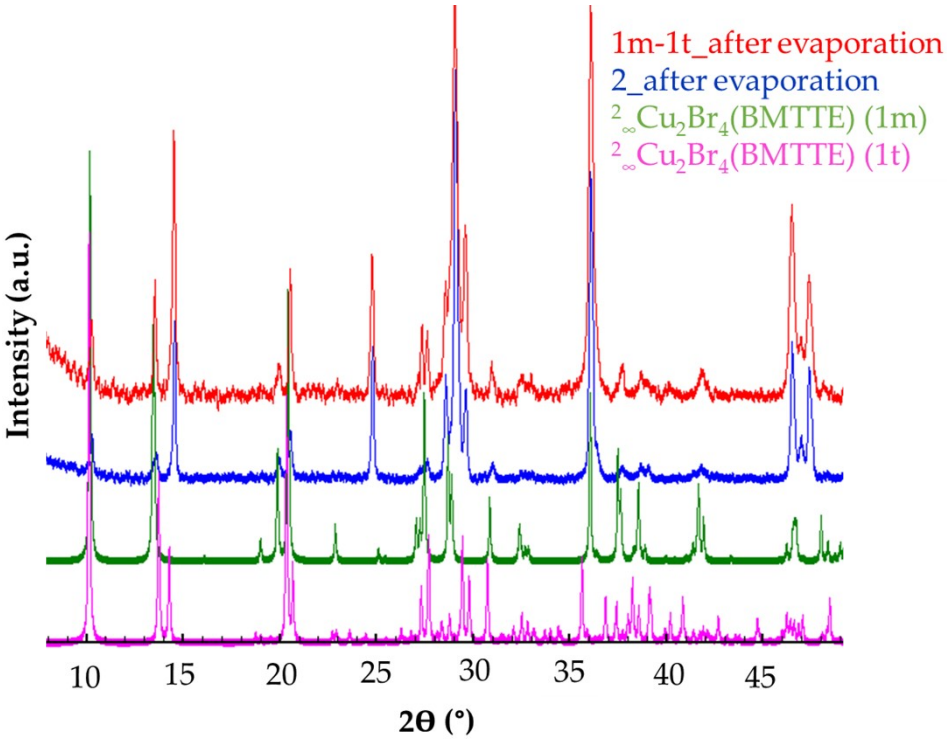

Figure S20: PXRD of each compound after water treatment compared with theoretical patterns of **1m** and **1t** Impurities are due to the presence of $CuBr_2$ salt.

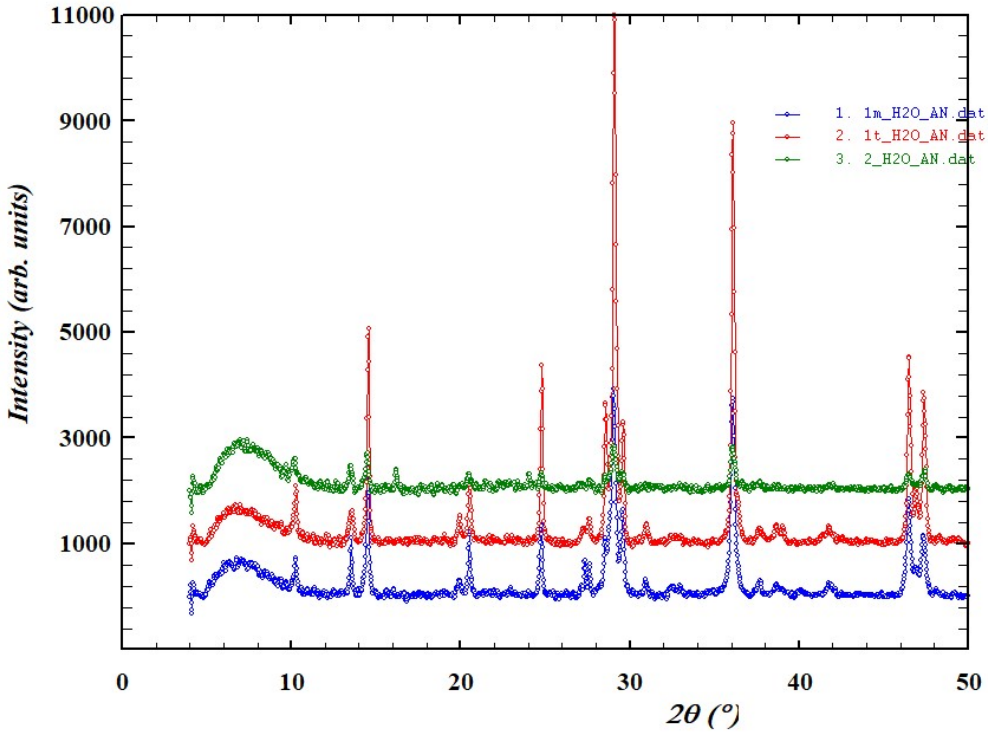

Figure S21: PXRD of resulting powder from **1m**, **1t** and **2** after water treatment.

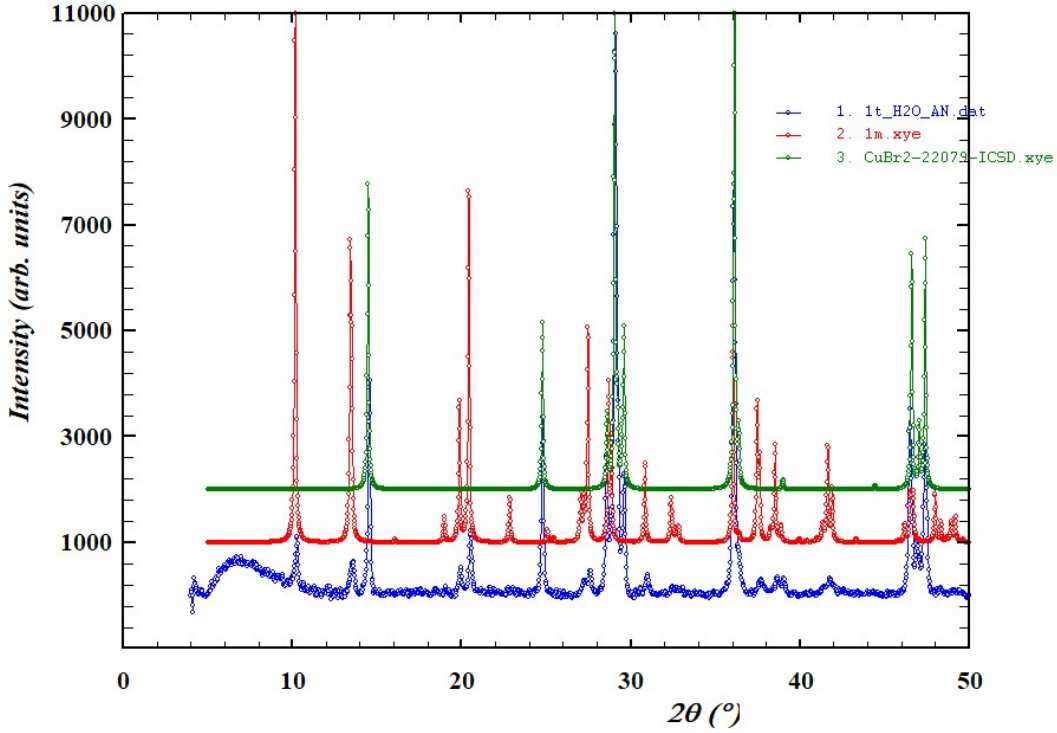

Figure S22: PXRD of **1t** after water treatment compared with the theoretical patterns of **1m** and **$CuBr_2$**

6. Reactivity of 2

METHOD A: Reaction with an excess of metal salt precursor.

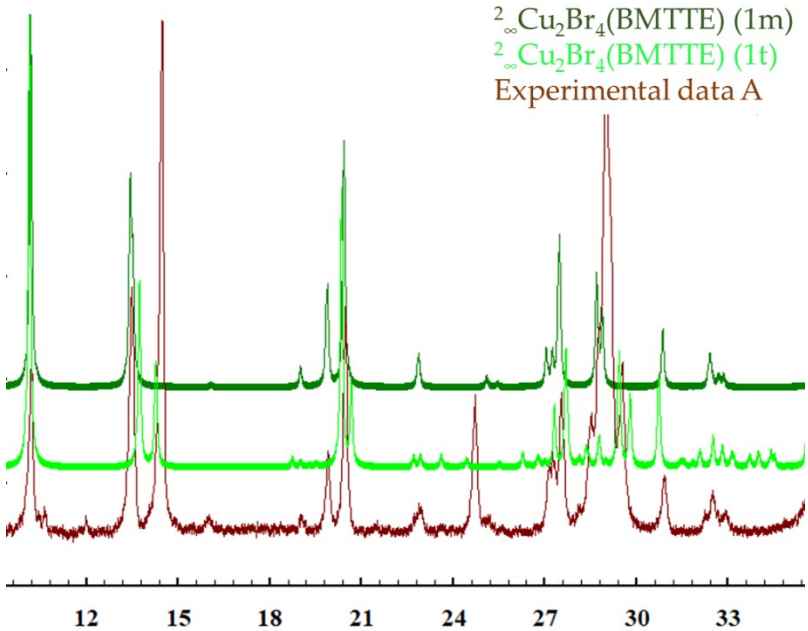

Figure S23: PXRD of reactivity of **2** in method A with theoretical of **1m** and **1t**.

Elemental analysis: Anal. Calc. for **2** + excess of $CuBr_2$ (2:9): 6.55%N, 4.21%C, 0.59%H, 3.75%S Found: 6.24%N, 4.54%C, 0.49%H, 4.12%S

METHOD B: Reaction with KI

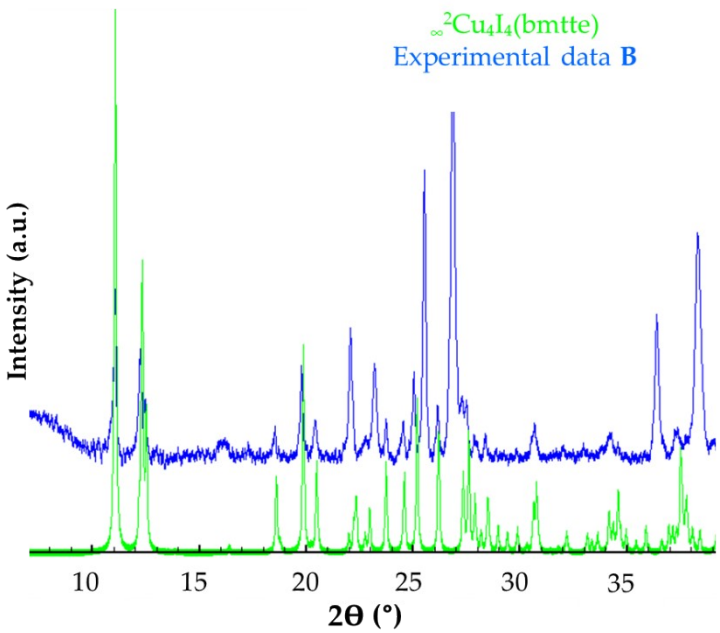

Figure S24: PXRD of reactivity of **2** in method B with theoretical of **4**.

Table S6*:* Elemental analysis**.** Experimental (Exp) and theoretical (Theo) % of N, C, H.

	Carbon (wt%)		**Nitrogen (wt%)**		**Hydrogen (wt%)**	
Compound	Exp	Theo	Exp	Theo	Exp	Theo
1m and 1t	9.71	10.22	14.91	15.89	1.25	1.43
2	14.98	14.03	22.62	21.82	2.04	1.96
3	13.73	13.22	20.97	20.55	1.72	1.85
4	7.21	7.08	11.09	11.01	1.01	0.99
2 + excess of $CuBr_2$ (2:9)	4.54	4.21	6.24	6.55	0.49	0.59

7. Redox behaviour of compounds 2 and 3

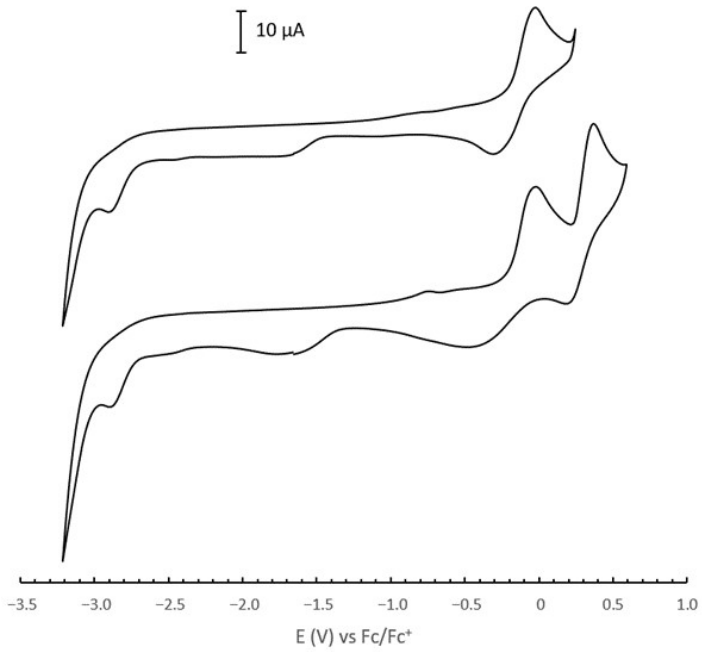

Figure S25: Cyclic voltammograms of 1 mM solution of complex **2** in DMSO, with 0.1 M TBAP as supporting electrolyte, at different potentials. Scan rate: 0.2 V/s.

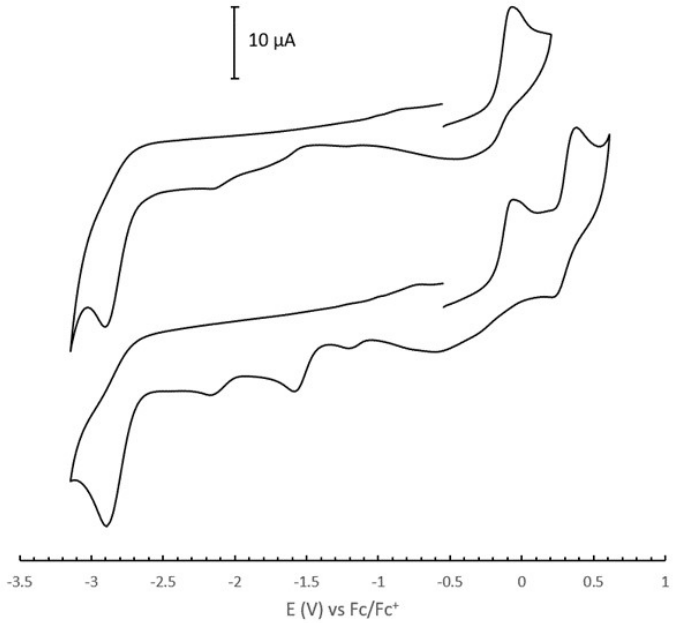

Figure S26: Cyclic voltammograms of 1 mM solution of complex **3** in DMSO, with 0.1 M TBAP as supporting electrolyte, at different potentials. Scan rate: 0.2 V/s.

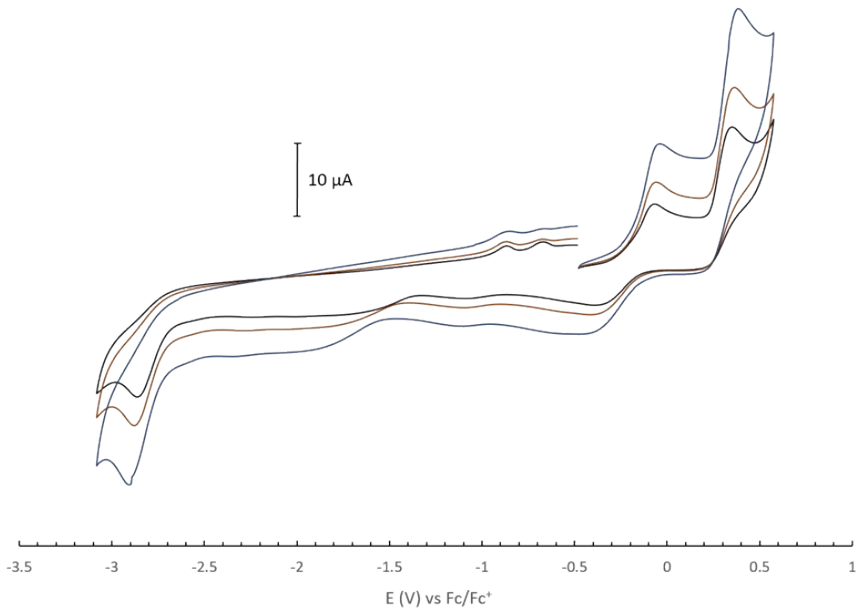

Figure S27: Cyclic voltammograms of 0.5 mM solutions of complex **2** in DMSO, with 0.1 M TBAP as supporting electrolyte, at different scan rates.

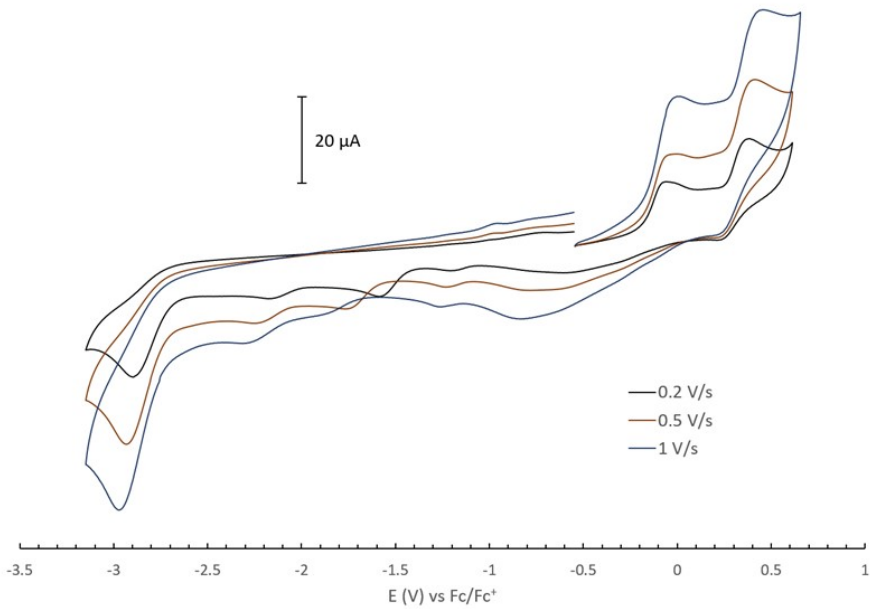

Figure S28: Cyclic voltammograms of 1 mM solutions of complex **3** in DMSO, at different scan rates.

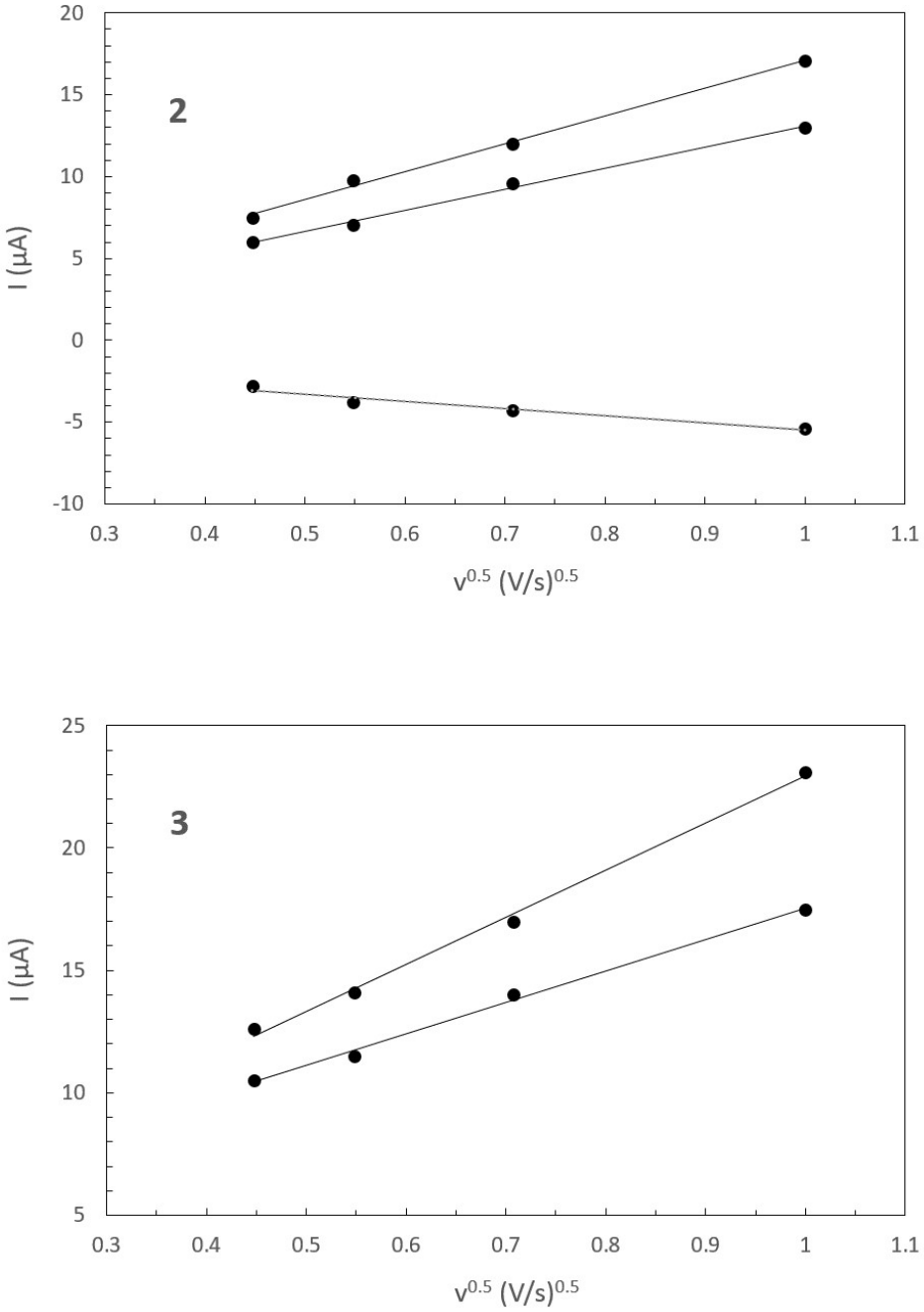

Figure S29. Graphical representation of the peak current vs the $v^{1/2}$ of complex **2** and **3.**